Investigation of the influence of design and material parameters in the progressive collapse analysis of RC structures

B. Santafé Iribarren [a,b], P. Berke [b], Ph. Bouillard [b], J. Vantomme [a], T.J. Massart [b,*]

[a] *Civil and Materials Engineering Dept., Royal Military Academy (RMA), Av. Renaissance 30, 1000 Brussels, Belgium*

[b] *Building, Architecture and Town Planning Dept. (BATir) CP 194/2, Université Libre de Bruxelles (ULB), Av. F.-D. Roosevelt 50, 1050 Brussels, Belgium*

Abstract

This contribution deals with the modelling of reinforced concrete (RC) structures in the context of progressive collapse simulations. One-dimensional nonlinear constitutive laws are used to model the material response of concrete and steel. These constitutive equations are introduced in a layered beam approach, in order to derive physically motivated relationships between generalised stresses and strains at the sectional level. This formulation is used in dynamic progressive collapse simulations to study the structural response of a multi-storey planar frame subjected to a sudden column loss (in the impulsive loading range). Thanks to the versatility of the proposed methodology, various analyses are conducted for varying structural design options and material parameters, as well as progressive collapse modelling options. In particular, the effect of the reinforcement ratio on the structural behaviour is investigated. Regarding the material modelling aspects, the influence of distinct behavioural parameters can be evaluated, such as the ultimate strain in steel and concrete or the potential material strain rate effects on the structural response. Finally, the influence of the column removal time in the sudden column loss approach can also be assessed. Significant differences are observed in terms of progressive failure pattterns for the considered parametric variations.

Key words: Progressive Collapse, Reinforced Concrete, Layered Beam, Strain Rate Effects, Finite Elements Method, Structural Dynamics

* Corresponding author.
Email address: thmassar@ulb.ac.be (T.J. Massart).

Engineering Structures, vol. 33(10), pp 2805-2820, 2011 *29 January 2014*

1 Introduction

Progressive collapse is a situation in which a local failure in a structure leads to a load redistribution, resulting in an overall damage to an extent disproportionate to the initial triggering event. Some examples of such a structural collapse occurred in the last decades, such as the Ronan Point apartment building in London, which partially collapsed in 1968 due to a gas explosion, or the Murrah Federal Building in Oklahoma City, which was destroyed in 1995 following the explosion of a bomb truck. Owing to the catastrophic nature of its consequences, progressive collapse has drawn an increasing interest in the civil engineering research community to derive new design rules.

Different simulation approaches dealing with the issue of progressive collapse can be found in the literature. This paper aims at contributing to the one referred to as the 'alternate load path' approach, which consists in considering stress redistributions throughout the structure following the loss of a vertical support element [1–3].

The recommendations for this approach presented by the United States Department of Defense (DoD) [2] and the General Services Administration (GSA) [3] suggest the use of step-by-step procedures for linear static, non-linear static and non-linear dynamic analyses. Other works propose static non-linear calculations accounting for dynamic inertial effects via load amplification factors for steel structures [4–8]. The DoD and GSA guidelines specify a dynamic load amplification factor of 2 to account for dynamic effects in static computations for both reinforced concrete and steel structures, which was considered to be highly conservative by some authors working on steel structures [5, 6, 8, 9, 11] and on reinforced concrete frames [10]; while insufficient for others whose research is focused on steel frames [12–14]. In order to obtain a systematic estimate of the dynamic load factors, equivalent static pushover procedures have been identified for steel structures, based on energetic considerations [5–8]. An optimisation approach based on nonlinear dynamic analyses was adopted in [8] in order to determine the most appropriate values for these factors, by performing a parametric study on topological variables for regular steel frames.

Apart from these equivalent quasi-static approaches, which constitute a major part of the related literature, non-linear dynamic procedures were recently conducted for both reinforced concrete and steel structures, to a variable extent of complexity [9–12, 14–22]. While in most of the recent works the structures are still modelled using 2D frames [9, 11, 12, 14, 19, 20], full non-linear 3D dynamic computations with geometrically nonlinear formulations are sometimes found in the literature related to steel structures [18, 22]. Nevertheless, such detailed approaches are scarce for reinforced concrete structures, partially due to the

high complexity involved in the modelling of the sectional response of heterogeneous RC beams. Hence, most of the progressive collapse related literature is focused on steel structures [4–9,11–14,18,20–23]. Fewer contributions tackle the dynamic analysis of progressive collapse of reinforced concrete structures, among which [10,15–17,19,24]. Recent works as [15–17] use an explicit finite element code, which is adopted in the simulation of blast-induced progressive collapse analyses, where the blast can be modelled in a sophisticated way (as a pressure wave propagation in the air) or in a more simplified manner (as a pressure-time distribution on the concerned elements). This computational technique is mainly suitable for modelling the high dynamic response of concrete and steel during the loading stage, due to the small time steps required by the explicit schemes. However, this event-modelling approach may become prohibited for large and/or finely discretised structures, due to its computational cost. As a result, the material modelling is often based on simplified approaches in which the modelling of the reinforced concrete response needs a priori postulated cross-sectional properties of beams requiring an identification of such generalised constitutive laws, as in [19]. In [24] the progressive collapse is simulated by using a plastic hinge formulation accounting for the steel bars yielding. A later work from the same author includes the steel bar fracture on a single beam test [25].

The purpose here is to analyse the structural response of a RC frame subjected to a sudden column loss. Such an abrupt member removal results in an impulsive loading scenario. This event-independent approach is widely used in the context of progressive collapse simulation techniques [2–12,14,18–22,26,27], with the aim of studying the structural resistance to the sudden loss of a primary load-bearing element, in contrast to the event-dependent approaches [15–17] where the collapse triggering event is modelled to analyse the structural response to a specific loading scenario. According to [26], the sudden column loss approach constitutes a useful design scenario for the assessment of structural robustness, since it offers an upper bound on the deformations obtained with respect to an event-dependent simulation approach.

The present contribution falls within the multi-level modelling of RC frames and uses a direct transition from the behaviour of concrete and steel at the constituent level to the response of the structural members at the structural level. A multilayered beam formulation [28–32] is adopted to this end, where the structural sections are discretised through a finite number of layers for which one-dimensional constitutive relations are described. This approach was used in the context of earthquake engineering for cyclic loading computations [29,30] or for the characterisation of a beam-column connection macromodel for progressive collapse simulations [19]. In [32] a layered model is developed to characterise the response of a simply supported RC slab to blast loadings.

However, to the best knowledge of the authors, a fully multilevel approach has

not yet been applied for the detailed modelling of reinforced concrete structures subjected to progressive collapse and hence constitutes a contribution to the study of this phenomenon. A geometrically linear formulation will be used, which seems acceptable in the framework of RC structures considering the rather small rotations involved due to the limited ductility of the sections. Nevertheless, the validity of such an assumption will be discussed in light of the results obtained. The complexity and computational cost of the methodology adopted here should be balanced with the objectives of the study. The present description enables a more realistic representation of the cross-sectional behaviour of reinforced concrete members where axial load-bending moment interactions are considered in combination with material nonlinearities, potentially including material rate effects. It also avoids the need to postulate closed-form relationships between generalised stresses and strains at the sectional level, preventing the related identification problem whenever the design and/or material parameters need to be modified or when a rate dependent approach is considered [33]. The complexity of quantifying the rotational capacity of RC members has been demonstrated in the literature. The ductility as the ability of the structure to redistribute moment and fail gradually is addressed in [34, 35]. In particular, the concrete softening is considered as an important component of the rotational capacity, which needs to be taken into account in order to ensure the ductility of RC structures. The multilayered approach adopted here allows for a gradual strength degradation as a consequence of the progressive failure of the constitutive layers, ensuring a proper account for the potential ductility of the RC members. Conversely, the advantages offered by the present formulation are counterbalanced by the higher computational cost required by a multiscale approach.

In this study, dynamic simulations are carried out on a two-dimensional representation of a reinforced concrete frame, modelled with multilayered beam elements and designed according to Eurocode 2 requirements [36]. The response of the frame when subjected to a sudden column loss, is then analysed. In order to assess the flexibility of this multiscale formulation, the influence of particular practical structural designs and material modelling options in the structural robustness is analysed. A strain rate dependent material approach will be developed as well to assess the level of dependence of the structural response on material strain rate effects.

The paper is organised as follows. In Section 2 the material behaviour of concrete and steel is described and the corresponding 1D constitutive models are proposed. The multilayered beam description used for the modelling of the reinforced beam elements is detailed, followed by the time integration scheme used for the dynamic computations. The application of the proposed methodology in the simulation of progressive collapse of RC structures is presented in Section 3, where a planar frame representing a building facade is subjected to a sudden column loss. A reference solution is obtained for a structure de-

signed according to the Eurocodes. This section also presents the results for varying material constitutive parameters of concrete and steel, namely the ultimate strains, which are varied in a realistic range of values obtained from the literature. Then, the influence of the reinforcement amount is analysed, by increasing the initial reinforcement ratios. As far as the technique of the sudden column loss simulation is concerned, the effect of the column removal time in the structural failure pattern is also assessed. The influence of the location of the removed column is studied, as well as the procedure adopted for the progressive collapse analysis (GSA vs. DoD). In Section 4 a material strain rate dependent formulation is described and the related results are compared to those obtained via the rate independent approach. Finally, a discussion is given in Section 5, along with some concluding remarks.

2 Rate independent modelling of RC structures

2.1 Material response of concrete and steel

The International Federation for Structural Concrete (*fib*) [37] describes the behaviour of concrete in compression as a stress-strain curve which depends on the concrete grade. The static compression curve is approximated by:

$$\frac{\sigma_{c,st}}{f_{c,st}} = -\frac{k\eta - \eta^2}{1 + (k-2)\eta} \text{ for } |\epsilon_c| < |\epsilon_{c,lim}| \tag{1}$$

in which $\sigma_{c,st}$ is the static compressive stress and ϵ_c the compressive strain. A C30 concrete type will be considered in the sequel with $f_{c,st}$ = 37.9 MPa the static compressive strength; k = 1.882 the plasticity number and $\eta = \epsilon_c/\epsilon_{c1}$, with ϵ_{c1} = -2.23‰ the strain at maximum stress. The parameters k and ϵ_{c1} are calculated as follows [37]:

$$k = \frac{E_c}{f_{c,st}/\,|\epsilon_{c1}|} \tag{2}$$

$$\epsilon_{c1} = -1.60 \left(\frac{f_{c,st}}{10^7}\right)^{0.25} \frac{1}{1000} \tag{3}$$

with E_c the Young's modulus.

In the present work, a bilinear stress-strain relationship is adopted for the sake of simplicity, as suggested in Eurocode 2 [36]. In Fig. 1 the simplified model used here is compared to the prescriptions of the *fib*, where the compressive stress-strain static curve is depicted. The assumed ultimate compressive strain is set to $\epsilon_{c,lim}$ = -0.35% [36], after which the stress vanishes, in order to

represent the failure of concrete in compression. The tensile contribution of concrete, being negligible with respect to the compressive response, will be ignored for the sake of simplicity.

For the steel reinforcement, a 500 MPa yield strength steel is employed. The simplified bilinear approach proposed by Eurocode 2 [36] is used as well. The evolution of the yield stress is modelled adopting a linear hardening approximation. The ultimate strain $\epsilon_{s,lim}$ is here taken equal to 4%, which corresponds to a steel ductility class between A and B [36]. In order to represent the failure of steel, the stress is set to zero for strains exceeding this value.

2.2 Constitutive equations: stress update algorithm

Based on the information reported in Section 2.1, a 1D elasto-plastic model is used for the behaviour of concrete and steel. The plastic domain is defined by an evolution law, which depends on the plastic strain history parameter κ, defined in a one-dimensional approach as

$$\kappa = \int \dot{\kappa} dt \text{ with } \dot{\kappa} = |\dot{\epsilon}^p| \tag{4}$$

with ϵ^p the plastic strain. This parameter κ actually consists of two terms, κ^t and κ^c controlling respectively the plastic flow in tension and in compression. The evolution law f is defined as:

$$f(\sigma, \kappa) = \begin{cases} \sigma - \bar{\sigma}_t(\kappa^t) \text{ for } \sigma \geq 0 \\ \sigma - \bar{\sigma}_c(\kappa^c) \text{ for } \sigma < 0 \end{cases} \tag{5}$$

where σ is the stress and $\bar{\sigma}_t$ and $\bar{\sigma}_c$ the tensile and compressive yield stresses, which depend on κ^t and κ^c respectively. If this dependence is nonlinear, a local Newton-Raphson scheme is used to determine the plastic state and the stress update. The stress update corresponding to an increment from state n to state $n+1$ can be written as:

$$\sigma_{n+1} = \sigma_n + E(\Delta\epsilon_{n+1} - \Delta\epsilon^p_{n+1}) \tag{6}$$

with E the elastic modulus, $\Delta\epsilon_{n+1}$ the strain increment and $\Delta\epsilon^p_{n+1}$ the plastic strain increment.

Eqs. (5) and (6) provide the set of constitutive expressions to be linearised at each iteration in a return-mapping algorithm in a general fashion:

$$\sigma_{n+1} - \sigma^{trial}_{n+1} + E\Delta\epsilon^p_{n+1} = 0 \tag{7}$$

$$f(\sigma_{n+1}, \kappa_{n+1}) = 0 \tag{8}$$

with $\sigma_{n+1}^{trial} = \sigma_n + E\Delta\epsilon_{n+1}$ the trial stress. By using (4), $\Delta\epsilon^p$ can be substituted in Eq. (7) and the constitutive problem can be expressed in a residual form as a function of two variables (σ and κ):

$$\{R(\sigma_{n+1}, \kappa_{n+1})\} = \left\{ \begin{array}{l} \sigma_{n+1} - \sigma_{n+1}^{trial} + E\Delta\kappa_{n+1} \\ \\ f(\sigma_{n+1}, \kappa_{n+1}) \end{array} \right\} = 0 \tag{9}$$

This system of equations is solved using a Newton-Raphson iterative scheme. Based on the linearised form of Eq. (9), the correction at iteration (j+1) is computed as:

$$\left\{ \begin{array}{l} \delta\sigma_{n+1} \\ \delta\kappa_{n+1} \end{array} \right\}_{j+1} = - \left[J_p\right]_j^{-1} \{R_j\} \tag{10}$$

where the Jacobian $[J_p]$ is defined as:

$$[J_p] = \frac{\partial \{R\}}{\partial \{\sigma, \kappa\}} \tag{11}$$

which can be used to evaluate the material tangent operator H consistent with the return-mapping algorithm:

$$H = \frac{\partial \sigma}{\partial \epsilon} \tag{12}$$

The constitutive parameters values used are shown in Table 1.

Table 1
Material parameters of the simplified bilinear model: in accordance with [36, 37]

concrete			steel			
$\bar{\boldsymbol{\sigma}}_{\boldsymbol{c}}$ [MPa]	$\boldsymbol{E_c}$ [GPa]	$\boldsymbol{\epsilon_{c,lim}}$	$\bar{\boldsymbol{\sigma}}_{\boldsymbol{0}}$ [MPa]	$\boldsymbol{E}$ [GPa]	$\boldsymbol{\epsilon_{s,lim}}$	$\bar{\boldsymbol{\sigma}}(\boldsymbol{\kappa})$ [MPa]
37.9	17	-0.35%	500	200	4%	$\bar{\sigma}_0(1 + 1.5\kappa)$

2.3 Layered beam formulation

A multilayered beam approach [28–32] is used for modelling the behaviour of the reinforced concrete members. Each cross-section where the beam response has to be computed – i.e. the integration points of a finite element – is discretised into a finite number of longitudinal layers where the 1D constitutive equations for concrete and steel are applied. The cross-sectional behaviour of the element is thus directly derived by integration of the stress-strain response

of the layers. According to Bernoulli's hypothesis the generalised stresses Σ^{gen} and strains E^{gen} read:

$$\{\Sigma^{gen}\} = \{N, M\} \tag{13}$$

$$\{E^{gen}\} = \{\bar{\epsilon}, \chi\} \tag{14}$$

with N the normal force, M the bending moment, $\bar{\epsilon}$ the axial strain and χ the curvature. Note that such averaged relations can only be applied in a point-wise manner in classical structural computations provided they do not exhibit overall softening, in order to keep a well-posed description. If softening is obtained in the beam response and unless a nonlocal or gradient type beam formulation is used, the corresponding dissipation at the structural scale is computationally determined by the element size [38, 39]. As a result, the structural discretisation will be chosen subsequently to provide localisation on a physically motivated beam length (size of the plastic hinges). This layered approach is summarised in Fig. 2, showing that only the longitudinal reinforcements are taken into account. The structural scale assumption (Bernoulli) remains consistent with this approach at the fine scale. As an additional simplifying assumption, a perfect bond is assumed between the layers. The element-wise stresses $\{\Sigma^{gen}\}$ are evaluated from the strains $\{E^{gen}\}$ at each integration point of the beam element as follows: first, the axial strains in each layer (ϵ_i) are computed,

$$\epsilon_i = \bar{\epsilon} - \bar{y}_i \chi \tag{15}$$

where $\bar{y}_i$ is the cross-sectional average vertical coordinate of layer i computed from the sectional center of gravity. Then the layer-wise stresses (i.e. the axial stresses σ_i) are obtained by applying the 1D constitutive equations on each layer. For the layers containing the steel reinforcements, the stresses in concrete and steel are computed separately and the layer average stress is obtained depending on the steel volume fraction of the considered layer. The stress is computed at the mid-height of the layer, and assumed to be constant over its thickness. Finally the cross-section generalised stresses $\{\Sigma^{gen}\}$ are evaluated by integrating the layer-wise one-dimensional stresses σ_i through the cross-sectional area of the beam:

$$\begin{aligned} N &= \sum \sigma_i \Omega_i \\ M &= -\sum \sigma_i \bar{y}_i \Omega_i \end{aligned} \tag{16}$$

with Ω_i the cross-sectional area of the layer. The related cross-sectional consistent tangent operator $[H_t]$ can be derived from the layer-wise consistent tangent operators H_i from Eq. (12) as follows:

$$[H_t] = \frac{\partial\{\Sigma^{gen}\}}{\partial\{E^{gen}\}} = \begin{bmatrix} \sum H_i \Omega_i & -\sum H_i \bar{y}_i \Omega_i \\ -\sum H_i \bar{y}_i \Omega_i & \sum H_i \bar{y}_i^2 \Omega_i \end{bmatrix} \tag{17}$$

Note that this approach allows for a gradual element-wise strength degradation as a consequence of the progressive failure of the constitutive layers, for which the stress is set to zero when the failure criteria are fulfilled. It allows for a ductile sectional response, which is proven to be an important factor for the moment redistribution in the structure [34, 35]. This also means that rather complex nonlinear sectional responses exhibiting softening can be obtained even with simplified 1D constitutive laws for the constituents (such as linear hardening) provided they are followed by a sudden drop of the stress at the ultimate strain. The straightforwardness of the present formulation to describe the RC sectional behaviour with respect to the closed-form approaches is pointed out.

2.4 Time integration scheme for the dynamic problem

An implicit Newmark scheme is adopted for the integration of the equations of motion in the simulations [40]. The discretised equations describing the equilibrium in dynamics read

$$\left\{f^{int}\left(\{q\}\right)\right\} + [M]\,\{\ddot{q}\} = \left\{f^{ext}\right\} \tag{18}$$

with $\{f^{int}\}$ the internal forces, $\{f^{ext}\}$ the external forces and $[M]$ the mass matrix. In the present paper, $[M]$ is considered to be constant while the internal forces $\{f^{int}\}$ are a nonlinear function of the displacements $\{q\}$. To solve Eq. (18) within an incremental-iterative scheme, a linearisation of the equations must be performed. Writing equilibrium as a residual form, the related structural Jacobian matrix $[J]$ is computed as the derivative of the residual with respect to the displacements:

$$[J] = \frac{\partial\left(\{f^{int}\left(\{q\}\right)\} + [M]\,\{\ddot{q}\} - \{f^{ext}\}\right)}{\partial\,\{q\}} \tag{19}$$

Using the notion of structural tangent operator $[K_t]$, which denotes the variation of the internal forces with respect to the displacements, the expression of the iteration matrix $[J]$ is given by:

$$[J] = [K_t] + [M]\,\frac{\partial\,\{\ddot{q}\}}{\partial\,\{q\}} \tag{20}$$

where $[K_t]$ is computed by applying the cross-sectional consistent tangent operator $[H_t]$ calculated in Eq. (17):

$$[K_t] = \sum_e \int_{V_e} [B]^t\,[H_t]\,[B]\,dV \tag{21}$$

where $[B]$ relates the generalised strains to the nodal displacements. Finally, the Newmark formulae allow computing the remaining term $\frac{\partial\{\ddot{q}\}}{\partial\{q\}}$ in Eq. (20), by defining relationships between the nodal displacements, velocities and accelerations. These formulae are expressed for a given time t_{n+1} as [40]:

$$\begin{aligned}\{\dot{q}_{n+1}\} &= \{\dot{q}_n\} + (1-\gamma)\Delta t\,\{\ddot{q}_n\} + \gamma\Delta t\,\{\ddot{q}_{n+1}\} \\ \{q_{n+1}\} &= \{q_n\} + \Delta t\,\{\dot{q}_n\} + \Delta t^2\left(\tfrac{1}{2}-\beta\right)\{\ddot{q}_n\} + \Delta t^2\beta\,\{\ddot{q}_{n+1}\}\end{aligned} \tag{22}$$

with Δt the time step; and γ and β the Newmark parameters associated with the quadrature scheme, which determine the stability of the method [40]. Considering these equations, the iteration matrix results in:

$$[J] = [K_t] + [M]\,\frac{1}{\beta\Delta t^2} \tag{23}$$

A numerical damping of 5% is introduced in order to reduce the spurious high frequency vibrations in the structural response, which significantly increase the computational time in large-scale calculations. The value of the Newmark's algorithm parameters γ and β are chosen such that this damping (affecting mainly the high frequency range) is provided in the simulation, while ensuring unconditional stability [40]:

$$\gamma = \frac{1}{2} + \alpha\ ;\quad \beta = \frac{1}{4}\left(\gamma + \frac{1}{2}\right)^2 \tag{24}$$

with $\alpha > 0$ the damping ratio, which is accordingly set to 0.05 in this case.

3 Numerical simulations for rate independent behaviour

3.1 Description of the RC planar frame subjected to column loss

Fig. 3 shows the structure under study, consisting of a two-dimensional representation of a five-storey eight-bay RC frame. The choice of this simplifying assumption (2D analysis) is justified by the conservative nature of the results obtained with such an approach with respect to full 3D computations, in which the transversal resistance would be considered. The floor span and height are 6 m and 3 m respectively, except for the ground floor which is 6 m high. The span in the perpendicular direction is 6 m. The columns and beams dimensions are 450×450 mm^2 and 600×450 mm^2 respectively. The envelope (vertical distance between the steel bars and the nearest section edge) is set to 5 cm for all the considered reinforcement schemes. The slab is 20 cm thick and an additional concrete layer of 10 cm is assumed. The floor does not provide

any resistance. The loads applied to the floor are those corresponding to the slab and beam weights as well as the live loads. The columns are subjected to their gravitational load. The minimal amount of reinforcement required for the beam sections has been obtained by way of the structural design analysis software Diamonds 2010 by Buildsoft [41], according to Eurocode 2 [36]. Three different sections have been obtained accordingly: one for the columns and two for the beams. Fully continuous bottom reinforcement is provided in the beams and 2/3 of the top reinforcement is made continuous as well, in order to ensure beam-to-beam continuity across the columns, which according to the GSA is essential for resisting the load reversals that follow the loss of a primary support [3]. Although transversal reinforcement is not explicitly represented, the structures under study will be considered to be properly designed against shear failure, as prescribed by the GSA [3], so that flexural effects are predominant in the beam response. The sectional dimensions and the reinforcing details are indicated in Fig. 4.

The purpose is to analyse the structural response of the frame when subjected to the sudden loss of its rightmost bottom column, which would correspond to a blast or impact loading scenario resulting in a full column removal. The sudden column loss technique is considered to offer a reasonable balance between the usefulness of the results and the computational effort to pay with respect to event-dependent approaches where the triggering event is explicitly modelled [26], including for instance horizontal loading due to the triggering event. This approximation is used here to keep the computational time acceptable, and to allow comparison with other approaches using this technique. Moreover, in [26] it was observed that the sudden column loss offered an upper bound on the structural deformation with respect to a more detailed approach where the blast loads were explicitly modelled. In practical terms, the sudden column loss technique employed here consists in erasing the column from the initial structural topology and replacing it by its resultant forces, applied with the regular loads in a first static loading step. The column resultant forces are subsequently removed (in a given removal time determined by the nature of the initial event: impact, blast...) while the regular loads are kept constant. This procedure preserves the real loading sequence. The GSA guidelines [3] specify a loading combination of

$$\text{Total Loads} = \text{Dead Loads} + 0.25\times\text{Live Loads}$$

to be applied for the dynamic simulation of progressive collapse. Therefore, 25% of the live loads are here applied. The resulting loads are indicated in Table 2.
The loading history used in the simulations is shown in Fig. 3: all the loads are applied to the structure in a sufficiently large time $t_0 = 60$ s for the loading to be considered static, since it prevents inertial effects from developing, as well as rate effects if they were considered. Then the member forces (R) are

Table 2
Loads applied to the beams (excluding self-weight).

Loads [kN/m]	Dead	Live	Total GSA	Total DoD
Floors	43.2	18	47.7	52.2
Roof	43.2	6	44.7	46.2

decreased to zero in a given removal time t_r and the response of the structure is observed over a time span of 2 s. Unless specified otherwise, the time step employed is $\Delta t = 5$ ms and the removal time t_r is also set to 5ms to simulate the instantaneous column loss representing the effect of a blast [42].

Two-noded Bernoulli beam elements with three integration points are used. A linear interpolation is used for the axial displacement, while a Hermite polynomial interpolation is used for the deflection. The cross-sectional discretisation – i.e. the thickness of the layers in the multilayered approach – is taken equal to 1cm. All computations are performed using a geometrically linear description. Since the energy dissipation depends on the discretisation adopted due to the softening nature of the problem [38, 39], here the beam elements have been given a length equal to 77% of the sectional height, so that localisation occurs on a region comparable to the corresponding characteristic plastic hinge length where most of the permanent beam rotation is known to be concentrated [34, 35].

To show the flexibility of the multilayered beam formulation to account for variations of the simulation parameters, as opposed to the approaches based on a priori postulated macroscopic cross-sectional response of the RC beams, the influence of particular design options and of material parameters in the rate independent structural response is analysed. In the first set of computations, the material parameters affecting the ultimate behaviour of concrete and steel are varied over the commonly used range found in the literature, to see their influence at the structural level. Note that these material variations, which may have a direct effect on the cross-sectional response, are naturally incorporated at the structural level thanks to the multilayered approach. This is in contrast with other simplified approaches in which the derivation of closed-form relationships between generalised stresses and strains requires an offline identification process whenever the material parameters are changed. The second set focuses on the variation of the design parameters. First, the effect of the amount of steel reinforcement is investigated. Then, the influence of the loading options is assessed: the value of the column removal time t_r is varied, so that the inertial effects in the overall response of the structure can be analysed. The influence of the topological location of the failing column is also investigated. Finally, the influence of the procedure chosen for progressive collapse verification (GSA vs. DoD) is studied. Table 3 summarises the values of these parameters for the different computations that constitute the present

study.

Table 3
Description of the tests.

Case	reinforcement	$\epsilon_{c,lim}$	$\epsilon_{s,lim}$	t_r [ms]	removed column	GSA/DoD
A	reference	-0.35%	4%	5	lateral	GSA
B	reference	-0.5%	4%	5	lateral	GSA
C	reference	-0.35%	10%	5	lateral	GSA
D	reference	-0.5%	10%	5	lateral	GSA
E	1.5×reference	-0.35%	4%	5	lateral	GSA
F	reference	-0.35%	4%	500	lateral	GSA
G	reference	-0.35%	4%	5	interior	GSA
H	reference	-0.35%	4%	5	lateral	DoD
I	reference	-0.35%	4%	5	interior	DoD

3.2 Reference solution (case A)

As previously mentioned, the structure under consideration has been designed to meet the requirements of the Eurocodes 2 and 3 in terms of minimal reinforcement amounts. Only 32mm diameter bars only have been used for the reference design (see details in Fig. 4), which results in a total reinforcement ratio of 1.6% for the columns, 0.6% to 0.9% for the beams in tension and 0.6% for the beams in compression. Fig. 5 depicts the results of the reference test at different times, counting from the onset of the column removal. A close-up view of the rightmost side of the structure is provided for the sake of clarity. The true-scale deformed shape of the structure is shown. The interpretation of the symbols employed to describe the failure pattern of the structure is summarised in Table 4: black dots (•) represent the plastification of the steel bars at the considered element; triangles (△) indicate that crushing of concrete in compression has occurred in less than one third of the element section (less than 1/3 of the concrete layers has reached the strain limit); squares (□) stand for concrete crushing in more than one third of the section; and crosses (×) represent the failure of the steel rebars and thus the final failure of the section. Note that the failure of a layer (reaching the ultimate strain in concrete or steel) does not stop curvature increment, but it eliminates the layer contribution to the cross-sectional strength. This allows for a gradual strength degradation through the section. This progressive degradation is also depicted for various sections of the structure: both for steel and for concrete, white indicates the areas that fall within the elastic range; red represents the zones

having reached the plastic domain; and black denotes material failure (the corresponding layer-wise stress has dropped to zero after the ultimate strain is reached). Tensile concrete is not depicted. It must be noted that the fully damaged elements are not removed from the topology. This means that the load transfer from potential fully failed elements to the neighbouring elements is not represented, since here the prime purpose is to study the ability of the structure to withstand the sudden column loss. As a result, the simulation is lead until a failure situation is detected, and the resulting mechanism is not modelled.

From the structural results in Fig. 5 it can be observed that failure progresses as follows: first the yielding of the tensile steel rebars occurs, followed by the crushing of concrete. Finally, the tensile rebars reach the ultimate strain causing the failure of the beam at the corresponding section. The progressive failure of the frame is restrained to the external bay initially supported by the removed column. Although failure does not spread beyond this region, the maximum allowable extent of collapse according to the GSA is exceeded since it should be "*confined to the structural bays directly associated with the instantaneously removed vertical member in the floor level directly above the instantaneously removed vertical member*" [3]. In the present case, all the floors above the failing column are included in the collapse region. As shown in Fig. 5, the complete failure of the exterior bay occurs 420 ms after the onset of the column removal. The amount of continuous reinforcement here provided seems insufficient to prevent progressive collapse for instantaneous removal of an exterior column.

Table 4
Interpretation of the structural failure symbols.

Symbol	Interpretation
•	Yielding of the steel rebars
△	Crushing of concrete in less than 1/3 of the section
□	Crushing of concrete in more than 1/3 of the section
×	Failure of the steel rebars

3.3 Influence of the material parameters

3.3.1 Ultimate strain of concrete and steel (cases B, C, D)

For a given, fixed design, it is important to assess the influence of material parameters for which varying values are found in the literature. The choice of such material parameters may indeed play an important role in the resul-

tant structural failure pattern. Hence, the sudden column loss is performed for different values of the ultimate strains of steel and concrete respectively. The reference ultimate strain of concrete in compression previously used is $\epsilon_{c,lim}$ = -0.35%, which corresponds to the most widely adopted value for unconfined concrete [36, 37]. However, the confining effect of the steel stirrups, which are not explicitly modelled in the present study, would induce an increase in the strain limit which depends on the lateral compressive stress and is often calculated as a function of the ratio of shear reinforcement [43]. Hence, the use of a higher value for the concrete strain limit is motivated in the present parametric study since it may result in an enhanced structural resistance to progressive collapse. On the other hand, a strain limit of $\epsilon_{s,lim} = 4\%$ is adopted for steel as a reference value, which would correspond to a ductility between classes A and B described in Eurocode 2 [36]. Higher values for this parameter may be used, matching a higher ductility class. The set of computations carried out is the following (Table 3): in the first one (case B) the ultimate strain of concrete is increased to $\epsilon_{c,lim}$ = -0.5% while the ultimate strain of steel is kept unvaried; in the second one (case C) the steel ultimate strain adopted is $\epsilon_{s,lim} = 10\%$ (resulting in a ductility class C according to Eurocode 2) and the concrete strain limit is kept equal to $\epsilon_{c,lim}$ = -0.35%; finally, the third computation (case D) is conducted for increased values of both limit strains: $\epsilon_{c,lim}$ = -0.5% in concrete and $\epsilon_{s,lim} = 10\%$ in steel. The results of the three computations are shown in Figs. 6 to 8.

The change of the ultimate strain of concrete by itself does not influence the global response, as can be seen in Fig. 6. It has a slightly delaying effect in the concrete crushing initiation. The crushed concrete area in the shown sections is slightly smaller than in case A. The complete failure of the rightmost bay takes place barely 10 ms later than in the reference test.

On the other hand, the increase of the strain limit of steel (Fig. 7) causes a significant delay on the appearance of failed sections. For instance, the final collapsed pattern is reached 885 ms after the onset of the column removal, which doubles the time required with respect to the reference case A. Note that the failing sections have more than one third of their concrete surface crushed before the failure of the tensile steel rebars takes place, which shows an increase in the efficiency of the RC sections since a better exploitation of the concrete in compression is achieved. This result indicates the important role that this parameter plays in the structural response.

If both parameters are increased simultaneously (Fig. 8), the structural collapse is prevented from occurring. The increased ductility of both materials leads to a structural strength gain, favoring the load redistributions. Fig. 11a shows the vertical displacement history of the node located at the connection with the removed column, as a function of the parameter combinations. The cross indicates the moment of collapse of the rightmost bay, when it occurs.

The increase of the ultimate strain for steel leads to a remarkably higher ductility at the structural scale, since the displacement at the moment of structural failure doubles the one obtained for the reference case A. For this particular case, results show that a computation including large displacements would be useful, contrarily to the previous tests where the displacements obtained can be considered small enough to neglect catenary effects.

3.4 Influence of the design parameters

3.4.1 Reinforcement ratio (case E)

The loss of the lateral ground column induces a sudden reversal of the bending moment in the central region of the supported beams, as well as a high increase of the bending moment at the connections with the adjacent internal columns. If these values of the bending moment were to be used for an elastic design of the collapse resistant structure, the originally calculated reinforcement ratios would have to be multiplied by a factor 3 or 4 in certain sections of the beams. A lower increase is however tested in this study, in order to remain in a reasonable range of reinforcement amount, which additionally allows for taking into account the load redistributions linked to the plastification of concrete and/or steel. Thus, the alternative design now considered is obtained by replacing the 32mm diameter bars by 40mm diameter ones, resulting in a reinforcing area of approximately 1.5 times the original one. The value of the resulting reinforcement ratios is now between 1% and 1.4% for the beams and 2.5% for the columns, falling within a range of values found in the literature [15, 17]. The response of the structure to the sudden column loss is shown in Fig. 9. As opposed to the reference results, this new design corresponding to an increased reinforcement area prevents collapse from happening. Plastification of the steel rebars is however observed in a few sections. The extra reinforcement applied, although much inferior to the one theoretically required for ensuring a collapse resistant (elastic) design, provides the necessary strength enhancement in the beam connections for the load redistributions to develop. Fig. 11b shows the vertical displacement of the node located just above the removed column connexion for the reference test and the test with increased reinforcement.

3.4.2 Influence of the column removal time (case F)

In this section, the interest is shifted towards the inertial effects in the progressive failure scheme of the structure. A larger column removal time is applied in order to represent a longer duration of the initial triggering event: $t_r = 500$ ms is now adopted, the order of magnitude of the time in which a column would

be removed in a low velocity impact event. This result is reported in Fig. 10. It shows that inertial effects play a major role in such a progressive collapse analysis: higher removal times, and subsequently lower accelerations, can lead to no collapse after the column loss. For the studied case, only plastification of the steel bars occurs at certain points. The vertical displacement history of the top node of the removed column is depicted in Fig. 11c, which has also been computed for two other removal times $t_r = 250$ ms and $t_r = 350$ ms. This illustrates to which extent the inertial effects affect the structural response and is consistent with the statement from [26], claiming that the sudden column loss idealisation (considering an instantaneous column removal) offers an upper bound on the deformations obtained through an event-dependent approach.

3.4.3 Influence of the removed column location (case G)

Finally, the effect of the topological location of the failing member is assessed by testing the sudden loss of an interior ground column. The material and modelling parameters are the reference ones. Fig. 12 summarises the response of the frame to the loss of the third ground column from the right.

Contrarily to the reference case A (Fig. 5), the frame resists to the sudden column loss. Although yielding of the steel rebars or even concrete crushing take place in some sections, complete failure is not observed in any of the beams. The damaged area in this case is also restrained to both bays directly associated with the failing column. The fact that an interior support is now removed results in an increased ability of the frame to redistribute loads among the remaining elements at both sides. This is made possible by the continuous bottom reinforcement provided in the beams, which is able to accommodate the bending moment reversal caused by the column removal.

3.4.4 Influence of the progressive collapse procedure (GSA vs. DoD) (cases H, I)

The DoD guidelines [2] propose a loading combination that includes 50% of the live loads instead of 25% as suggested by the GSA [3]. Thus the total downward loads applied are

$$\text{Total Loads} = \text{Dead Loads} + 0.5\times\text{Live Loads}$$

and are indicated in Table 2. This analysis procedure is now adopted to simulate the sudden column loss. The results for an exterior column removal (case H) are depicted in Fig. 13. The total failure of the rightmost bay takes place about 100 ms earlier than in the reference case (Fig. 5). Apart from this fact, no significant difference is found between both results.

On the contrary, if an interior column removal is considered (case I), as shown in Fig. 14, the results differ substantially from the ones previously obtained via the GSA specifications (Fig. 12). The collapse of the two bays directly associated with the removed column occurs now that 50% of the live loads are applied. Fig. 15 depicts the displacement history for cases H and J. This indicates that the results obtained in a sudden loss analysis may differ depending on the procedure standards considered, even for the most widely used methods, which shows the importance of the procedure used for the simulation of progressive collapse.

4 Investigation of the strain rate effects

4.1 Strain rate effects in RC

For a wide range of triggering events (impact, blast...), progressive collapse is a dynamic process involving rather high strain rates. As a result, the global response of a part or the entire structure is likely to entail dynamic effects, as well as nonlinear effects in the material response. Reinforced concrete structures subjected to high loading rates are expected to have a different response than when loaded statically. For instance, concrete shows a strongly rate dependent behaviour, with both compressive and tensile strengths increasing significantly with the strain rate [37,44,45], as confirmed by experimental tests carried out by means of the Split Hopkinson Bar [46,47]. Steel also presents a strain rate sensitive behaviour, although to a lower extent than concrete [48]. Since the progressive collapse related structural behaviour considerably depends on stress redistributions, this material strain rate dependence, leading to a enhancement in the local strength with increasing strain rates, might also induce a different overall response of the whole structure. The multilayered beam formulation can help in assessing the need for such a modelling tool. It indeed allows for the incorporation of the rate effects at the sectional level linking the generalised stresses (N and M) to the generalised strains ($\bar{\epsilon}$ and χ) and their rates ($\dot{\bar{\epsilon}}$ and $\dot{\chi}$) implicitly; thereby avoiding a complex identification of closed-form rate dependent sectional evolution laws.

Numerous references on the rate-dependent behaviour of concrete can be found in the literature [49–51], where the strength enhancement at the material level is studied and modelled in the context of small scale structural computations. However, the influence of the viscous effects at the global scale has not yet been investigated in contributions related to structural progressive collapse. Here, the rate dependent effects are incorporated from the rate dependence at the material level using the layered beam approach.

The International Federation for Structural Concrete (*fib*) [37] describes the rate dependent behaviour of concrete in compression by means of a rate dependent modulus of elasticity and the so-called dynamic increase factors (DIF) on strength, representing the ratio of dynamic to static strength, as determined by Malvar and Crawford [45]. The effect of strain rate on Young's modulus and the dynamic increase factors are estimated by [45]:

$$\frac{E_c}{E_{c,st}} = \left(\frac{\dot{\epsilon}}{\dot{\epsilon}_{st}}\right)^{0.026} \tag{25}$$

$$DIF = \frac{f_c}{f_{c,st}} = \begin{cases} \left(\frac{\dot{\epsilon}}{\dot{\epsilon}_{st}}\right)^{1.026\alpha_s} & \text{for } \dot{\epsilon} \leq 30s^{-1} \\ \gamma_s \left(\frac{\dot{\epsilon}}{\dot{\epsilon}_{st}}\right)^{1/3} & \text{for } \dot{\epsilon} > 30s^{-1} \end{cases} \tag{26}$$

where E_c is the compressive Young's modulus at strain rate $\dot{\epsilon}$; $E_{c,st}$ the compressive static Young's modulus; f_c the compressive strength at strain rate $\dot{\epsilon}$; $f_{c,st}$ the static compressive strength (37.9 MPa for a C30 concrete); $\dot{\epsilon}$ a strain rate between $3 \cdot 10^{-5}$ s^{-1} and 300 s^{-1}; $\dot{\epsilon}_{st}$ the compressive 'static' strain rate of $3 \cdot 10^{-5}$ s^{-1}; $log(\gamma_s) = 6.156\alpha_s - 2$; $\alpha_s = 1/(5 + 9f_{c,st}/10^7)$.

Based on these dynamic increase factors, a strain rate dependence is introduced both in the elastic and in the plastic domain, to match the *fib* description in terms of peak stress, strain at peak stress and ultimate strain. This allows for preserving the crushing energy (area under the compressive stress-strain curve) as shown in Fig. 16a, where the simplified model used here is compared to the prescriptions by the *fib*. The compressive stress-strain curves for a C30 concrete type are depicted for various strain rates. The rate dependent curves suggested by the *fib* have been constructed following the static stress-strain expression based on relations (1), (2) and (3), and the DIFs from Eq. (26). A rate dependent Young's modulus is hence adopted, an important feature due to its influence in the load redistributions involved in progressive collapse analyses. The ultimate compressive strain (-0.35%) corresponding to the crushing strain of concrete will be considered constant independently of the strain rate, as no evolution of this parameter was evidenced in [52]. The dynamic increase factors for a C30 concrete type obtained with the proposed model are in good agreement with the prescriptions of the *fib* [37], as observed in Fig. 17a.

For steel, Young's modulus is assumed to be rate independent, as observed by [48]. The DIFs corresponding to the yield stress for steel obey the following expression according to [48]:

$$DIF_{steel} = \frac{f_y}{f_{y,st}} = \left(\frac{\dot{\epsilon}}{\dot{\epsilon}_{st}}\right)^{\alpha} \tag{27}$$

with f_y the yield stress at strain rate $\dot{\epsilon}$; $f_{y,st}$ the static yield stress (here 500 MPa); $\dot{\epsilon}$ a strain rate between 10^{-4} s^{-1} and 225 s^{-1}; $\dot{\epsilon}_{st}$ the 'static' strain rate of 10^{-4} s^{-1}; $\alpha = 0.074 - 0.040 f_y/414$. As for concrete, the model is adjusted to match the results in [48] in terms of DIFs. The ultimate strain, which is not observed to vary as a function of the strain rate [48], is here taken equal to 4%. In order to represent the failure of steel, the stress is set to zero for strains exceeding this value, independently of the value of strain rate. Fig. 16b shows the rate dependent stress-strain curves. The DIFs are depicted in Fig. 17b.

4.3 Rate dependent constitutive model

A natural way to include the strain rate effects in a material model is the introduction of viscous terms in the constitutive law. For instance, Pedersen et al. [49] developed a rate dependent macroscopic material model based on the microscopic and mesoscopic behaviour of concrete. In the present contribution, rate dependent one-dimensional constitutive laws for concrete and steel are used in the layers of the layered beam model. Perzyna's viscoplastic model [53, 54] is adopted for the behaviour of both constituents. The viscoplastic strain rate $\dot{\epsilon}^{vp}$ is expressed as a function of the yield function f defined in Eq. (5):

$$\dot{\epsilon}^{vp} = \frac{1}{\eta} \left\langle \frac{f}{\bar{\sigma}_0} \right\rangle^N \frac{df}{d\sigma} \tag{28}$$

where $\bar{\sigma}_0$ is the initial yield stress; f is the yield function which accounts for the overstress $(\sigma - \bar{\sigma})$, since here the applied stress can exceed the yield stress contrarily to the rate independent plastic case; η and N are viscosity parameters, with $N \geq 1$ an integer number; and $\langle\ \rangle$ denotes the Macaulay brackets. Note that the parameter η depends on the strain rate $\eta(\dot{\epsilon})$ to match the material response reported in the literature in terms of DIFs [37, 45, 48]. Rewriting Eq. (28) in an incremental fashion, the residual in Eq. (9) now reads:

$$\{R(\sigma_{n+1}, \kappa_{n+1})\} = \left\{ \begin{array}{l} \sigma_{n+1} - \sigma_{n+1}^{trial} + E(\dot{\epsilon}_{n+1}) \Delta\kappa_{n+1} \\ \\ \eta(\dot{\epsilon}_{n+1}) \Delta\kappa_{n+1} - \Delta t_{n+1} \left\langle \frac{f(\sigma_{n+1}, \kappa_{n+1})}{\bar{\sigma}_0} \right\rangle^N \left. \frac{df}{d\sigma} \right|_{n+1} \end{array} \right\} \tag{29}$$

where Eq. (4) and the approximation $\dot{\kappa} = \Delta\kappa/\Delta t$ have been used, with Δt the time step. Note that now the rate dependence also needs to be introduced in the Young's modulus $E(\dot{\epsilon})$ for concrete, to obtain a strain at peak stress that matches the previsions reported in [37], as shown in Fig. 16a. The values of the viscoplastic model parameters are given in Table 5. The rate dependent parameters $E_c(\dot{\epsilon})$, $\eta_c(\dot{\epsilon})$ and $\eta_s(\dot{\epsilon})$ are depicted in Fig. 18. A perturbation tech-

Table 5
Viscoplastic model parameters

concrete			steel	
$\boldsymbol{E_c}$ [GPa]	$\boldsymbol{N_c}$	$\boldsymbol{\eta_c}$ [$\mathbf{s^{-1}}$]	$\boldsymbol{N_s}$	$\boldsymbol{\eta_s}$ [$\mathbf{s^{-1}}$]
$E_c(\dot{\epsilon})$ (Fig.18a)	1	$\eta_c(\dot{\epsilon})$ (Fig.18b)	1	$\eta_s(\dot{\epsilon})$ (Fig.18c)

nique is used to evaluate the material tangent operator H consistent with the return-mapping algorithm. This avoids the analytical derivation of the constitutive equations with respect to the strain ϵ, a non-trivial task due to the strain rate dependence of the parameters $E_c(\dot{\epsilon})$, $\eta_c(\dot{\epsilon})$ and $\eta_s(\dot{\epsilon})$.

The introduction of the previous rate dependent constitutive equations $\sigma(\epsilon, \dot{\epsilon})$ in the layered beam formulation provides rate dependent relations between the beam generalised stresses and strains. To obtain such relationships, the layer-wise strain rates are computed from the generalised strain rates $\{\dot{E}^{gen}\} = \{\dot{\bar{\epsilon}}, \dot{\chi}\}$ as:

$$\dot{\epsilon}_i = \dot{\bar{\epsilon}} - \bar{y}_i \dot{\chi} \tag{30}$$

An analytical version of such a rate dependent multilayered approach was used in [32], where the strain rate dependence is introduced in a simply supported RC slab under blast loading by multiplying the layer-wise stresses $\sigma_i(\epsilon_i)$ by their corresponding dynamic increase factors $\mathrm{DIF}(\dot{\epsilon}_i)$. Contrarily to the present work, the rate dependence of concrete in the elastic region was however not taken into account.

At the structural scale, the equilibrium equations now read:

$$\left\{f^{int}\left(\{q\}, \{\dot{q}\}\right)\right\} + [M]\{\ddot{q}\} = \left\{f^{ext}\right\} \tag{31}$$

where $\{f^{int}\}$ is also a function of the displacement rates $\{\dot{q}\}$:

$$\left\{f^{int}\left(\{q\}, \{\dot{q}\}\right)\right\} = \sum_e \int_{V_e} [B]^t \left\{\Sigma^{gen}\left(\{E^{gen}\}, \{\dot{E}^{gen}\}\right)\right\} dV \tag{32}$$

Note that the structural tangent matrix $[K_t]$ from Eq. (21) now contains inherent rate dependent damping terms stemming from the rate dependence of the internal forces. This means that the strain rate dependent nature of the material constitutive equations provides a certain amount of damping at the structural level, as opposed to rate independent approaches.

4.4 Rate dependent simulation of progressive collapse

The sudden column loss simulation is now performed using the previously described strain rate dependent approach. This is done for two different removal

times $t_r = 5$ ms and $t_r = 500$ ms, which determine the extent of the strain rate effects in the structural response. Results are shown in Figs. 19 and 20 respectively. For instance, if a removal time $t_r = 5$ ms is applied, the material strength-enhancing strain rate effects prevent collapse from happening, as opposed to the rate independent case (case A) where the entire rightmost bay collapses. It must be noted that, for the studied reinforcement arrangement, this structural enhancement is mostly provided by the rate dependence of the steel bars, since the amount of reinforcement is similar at both sides (upper and lower) for the sections considered here. The contribution of the concrete rate dependence to this improved structural response is thus lower. For a removal time of $t_r = 500$ ms, the structure does not collapse either, as it was also the case in the rate independent approach (case F). The comparison of both results with respect to the rate independent case in terms of vertical displacements is shown in Fig. 21. It can be observed that taking the strain rate effects in consideration results in a structural integrity improvement. If the column removal is performed in a larger timespan $t_r = 500$ms, the strain rate effects become less significant. In this case, the difference between the rate dependent and the rate independent approaches is lower: the final response patterns are similar. The classically adopted rate independent approach thus leads to a more important damage evolution as the removal time decreases, due to the increase of the inertial effects: while the inertial effects favor the propagation of the failure in the structure, the strain rate effects limit the degree of failure. Nevertheless, the results obtained confirm that the use of the sudden column loss idealisation (where an instantaneous removal of the column is assumed) to obtain an upper bound on the deformation demands [26] is also applicable to the rate dependent case.

5 Discussion and concluding remarks

A multilayered beam element was developed to simulate the dynamic response of RC structures subjected to a sudden column loss. Due to the quasi-instantaneous character of the column removal (which takes place in a single time step, i.e. 5 ms), a loading scenario in the impulsive range is considered here. A nonlinear model was adopted for the material behaviour of concrete and steel. This multilevel approach allows for a direct transition between the material constitutive equations and the response at the structural level, providing physically motivated relationships between the generalised stresses and the generalised strains. More importantly, a strain rate dependent material formulation has also been developed. The rate dependence is introduced in both the elastic and the plastic behaviors. The sudden column loss methodology has been applied for a structure designed according to the Eurocodes prescriptions. A study was conducted by varying some design and material

parameters in a commonly used range to analyse their effect on the obtained collapse patterns. The following conclusions may be drawn:

(1) As expected, the design options have an important effect on the progressive collapse response of a structure: an increase of 50% on the initial reinforcement amount shows a significant increased resistance to the sudden column loss in the studied structure.
(2) While the ultimate strain of concrete does not appear to be decisive in the progressive collapse mechanism, the ultimate strain of steel might be determinant to the point that collapse can be avoided by increasing the value of this parameter in a realistic range. Moreover, higher values of the ultimate strain of steel lead to a much more ductile structural response.
(3) The column removal time is also determinant in the structural response, since the inertial effects are directly related to this variable: for higher removal times the accelerations involved in the process are smaller and thus the extent of structural damage is lower. This confirms that the sudden column loss idealisation represents a useful design scenario for the assessment of structural robustness [26].
(4) The location of the removed element also has an effect on the propagation of collapse: the removal of an interior column leads to lower degrees of structural damage, due to the support provided by the neighboring column at both sides.
(5) The procedure used for the simulation of the sudden column loss (GSA or DoD) has a significant effect on the results: the DoD procedure, which considers 50% of the live loads, might lead to conservative designs with respect to the GSA guidelines, which suggests including only 25% of the live loads in the computations.
(6) The strain rate effects in the sudden column loss simulation have been proven to be potentially significant at the structural level. The strength enhancement which stems from the material level results in a structural integrity improvement for the studied structure. This structural enhancement is mostly provided by the rate dependence of the steel bars due to the particular reinforcement arrangement adopted here.

Various simplifications have been adopted for the present study, for which a discussion is presented next. First, a planar representation of the structure has been employed as an initial approach to the problem. Note that the single column removal in a two-dimensional representation would correspond to removing a whole row of columns in 3D since the transversal resistance is not taken into account. This simplified approach might thus lead to conservative results. The extension to a three-dimensional approach seems to be the logical next step in order to obtain a more realistic structural response. However, this extension is nontrivial both from the computational cost viewpoint, and from the perspective of structural complexities (representation of torsional effects, stiffening effects of the floors...). Secondly, the geometrically linear formulation

adopted here is partially justified by the small-range displacements obtained in most of the computations. Nevertheless, a large displacement analysis is foreseen for forthcoming works even though this issue is out of scope of the present paper. Third, the shear reinforcements have not been explicitly modelled. An implicit, phenomenological way of taking them into account has been considered by increasing the concrete ultimate strain. The results however showed no significant differences in the structural response. Moreover, the Bernoulli beam approximation adopted in the present formulation is unable to account for the shear deformation, since the cross-sections remain plane and perpendicular to the longitudinal axis of the beam. This choice, which implies that shear failure is not considered, was justified by the fact that the structures under study are considered to be properly designed against shear failure (as prescribed by the GSA [3]) so that flexural effects are predominant in the beam response. In order to obtain a more complete approach, in which different failure modes could be incorporated, the upgrade to a Timoshenko beam element formulation would be recommended as in [30] where the formulation of a Timoshenko multifiber beam element was elaborated and applied for a small-scale analysis. The proper modelling of shear failure would however require in addition a shear failure criterion based on the layered beam approach results, a non trivial extension. Finally, the failed elements are not removed from the topology and thus remain attached to the structure after reaching complete failure, keeping transferring stresses to the intact elements in the vicinity. As a consequence, the impact of failing members on adjacent elements is not included, ignoring the corresponding dynamic load transfer. The sudden column loss approximation was used in the present study, with the purpose of analysing the progressive spread of damage in the structure after localised failure has occurred, since all the potential sources of collapse initiation cannot be investigated. A detailed characterisation of this triggering event would offer the most realistic solution, in which the full dynamic character of the triggering event would be included, incorporating potential horizontal components of the triggering event. However, the computational time required would be prohibitive, due to the small step size needed for a thorough simulation of a short-time duration event. The sudden column loss technique is considered to offer a reasonable balance between the usefulness of the results and the computational effort.

In spite of the aforementioned simplifying assumptions, the effects observed with the present approach are supposed to remain general and are expected to be reproduced in a more complete approach. Moreover, the versatility of the present multilevel methodology must be underlined: it provides a more realistic representation of the cross-sectional response of reinforced concrete members where axial load-bending moment interactions are naturally included, avoiding the need to postulate approximate closed-form relationships between generalised stresses ans strains. It offers an increased flexibility with respect to other approaches, for which any material and/or design parametric variation would

require an offline identification process to derive analytical expressions. In the present formulation, these variations are naturally introduced in the structural response. Furthermore, it can be extended to other fine-scale constitutive laws, including a different material response and/or additional modelling features such as damage, a particularly meaningful feature of the material response under cyclic loading. Additionally, the present multilevel approach could be considered as a complement to other simplified methodologies such as the one proposed in [6,7], in order to overcome the high computational effort involved in the proposed detailed approach. In these contributions, the authors present a multi-level framework for progressive collapse assessment of structures subject to sudden column loss which allows including various levels of structural modelling sophistication: both detailed and simplified approaches can be combined according to the level of structural idealisation considered. Instead of using a nonlinear dynamic finite element analysis, the nonlinear static response is only analysed and the dynamic effects are evaluated in a simplified manner. Such a strategy which allows a significant reduction of the computational time could be combined with the material and/or design sensitivity issues studied in the present analysis (potentially including the material rate dependence) to yield additional practical rules for design.

Acknowledgements

The research presented in this paper is supported by the Belgian Ministry of Defence (project DY-03) for the first author. Financial support from the F.R.S.-FNRS under grants 1.5.032.09. F and 2.4.513.09. F (FRFC) for the last author and under grant 1.2.093.10. F for the second author is gratefully acknowledged.

References

[1] Ellingwood B, Leyendecker E. Approaches for design against progressive collapse. J Struct Div-ASCE 1978;104(ST3):413–23.

[2] Department of Defense (DoD). Unified Facilities Criteria (UFC): Design of buildings to resist progressive collapse, UFC 4-023-03. Washington DC; 2009.

[3] United States General Services Administration (GSA). Progressive collapse analysis and design guidelines for new federal office buildings and major modernization projects. Washington DC; 2003.

[4] Grierson DE, Xu L, Liu Y. Progressive-failure analysis of buildings subjected to abnormal loading. Comput-Aided Civ Inf 2005;20:155–71.

[5] Vlassis AG, Progressive collapse assessment of tall buildings. Ph.D. thesis, Department of Civil and Environmental Engineering, Imperial College London; 2007.

[6] Izzuddin BA, Vlassis AG, Elghazouli AY, Nethercot DA. Progressive collapse of multi-storey buildings due to sudden column loss - Part I: Simplified assessment framework. Eng Struct 2008;30:1308–18.

[7] Izzuddin BA, Vlassis AG, Elghazouli AY, Nethercot DA. Progressive collapse of multi-storey buildings due to sudden column loss - Part II: Application. Eng Struct 2008;30:1424–38.

[8] Menchel K, Progressive collapse: comparison of main standards, formulation and validation of new computational procedures. Ph.D. Thesis, Université Libre de Bruxelles. Belgium; 2008.

[9] Kim J, Kim T. Assessment of progressive collapse-resisting capacity of steel moment frames. J Constr Steel Res 2009;65:169–79.

[10] Tsai M-H, Lin B-H. Investigation of progressive collapse resistance and inelastic response for an earthquake-resistant RC building subjected to column failure. Eng Struct 2008;30:3619–28.

[11] Kaewkulchai G, Williamson EB. Dynamic behaviour of planar frames during Progressive Collapse. 16th ASCE Engineering Mechanics Conference. University of Washington. Seattle, USA; 2003.

[12] Kaewkulchai G, Williamson EB. Beam element formulation and solution procedure for dynamic progressive collapse analysis. Comput Struct 2004;82:639–51.

[13] Ruth P, Marchand KA, Williamson EB. Static equivalency in progressive collapse alternate path analysis: reducing conservatism while retaining structural integrity. J Perform Constr Fac 2006;20(4):349–64.

[14] Kim H-S, Kim J, An D-W. Development of integrated system for progressive collapse analysis of building structures considering dynamic effects. Adv Eng Softw 2009;40:1–8.

[15] Luccioni BM, Ambrosini RD, Danesi RF. Analysis of building collapse under blast loads. Eng Struct 2004;26:63–71.

[16] Weerheijm J, Mediavilla J, van Doormaal JCAM. Explosive loading of multi storey RC buildings: Dynamic response and progressive collapse. Struct Eng Mech 2009;32(2):193–212.

[17] Shi Y, Li Z-X, Hao H. A new method for progressive collapse analysis of RC frames under blast loading. Eng Struct 2010;32:1691–1703.

[18] Kwasniewski L. Nonlinear dynamic simulations of progressive collapse for a multistory building. Eng Struct 2010;32:1223–35.

[19] Bao Y, Kunnath SK, El-Tawil S, Lew HS. Macromodel-based simulation of progressive collapse: RC frame structures. J Struct Eng-ASCE 2008;134(7):1079–91.

[20] Khandelwal K, El-Tawil S, Sadek F. Progressive collapse analysis of seismically designed steel braced frames. J Constr Steel Res 2009;65:699–708.

[21] Fu F. Progressive collapse analysis of high-rise building with 3-D finite element modeling method. J Constr Steel Res 2009;65:1269–78.

[22] Galal K, El-Sawy T. Effect of retrofit strategies on mitigating progressive collapse of steel frame structures. J Constr Steel Res 2010;66:520–31.

[23] Vlassis AG, Izzuddin BA, Elghazouli AY, Nethercot DA. Progressive collapse of multi-storey buildings due to failed floor impact. Eng Struct 2009;31(7):1522–34.

[24] Sasani M, Sagiroglu S. Gravity Load Redistribution and Progressive Collapse Resistance of 20-Story Reinforced Concrete Structure following Loss of Interior Column. ACI Struct J 2010;107(6):636–44.

[25] Sasani M, Werner A, Kazemi A, Bar fracture modeling in progressive collapse analysis of reinforced concrete structures. Eng Struct 2011;33(2):401-9.

[26] Gudmundsson GV, Izzuddin BA. The 'sudden column loss' idealisation for disproportionate collapse assessment. The Structural Engineer 2008;88(6):22–6.

[27] Menchel K, Massart TJ, Rammer Y, Bouillard P. Comparison and study of different progressive collapse simulation techniques for RC structures. J Struct Eng-ASCE 2009;35(6):685–697.

[28] Anthoine A, Guedes J, Pegon P. Non-linear behaviour of reinforced concrete beams: from 3D continuum to 1D member modelling. Comput Struct 1997;65(6):949–63.

[29] Davenne L, Ragueneau F, Mazars J, Ibrahimbegovic A. Efficient approaches to finite element analysis in earthquake engineering. Comput Struct 2003;81:1223–39.

[30] Mazars J, Kotronis P, Ragueneau F, Casaux G. Using multifiber beams to account for shear and torsion. Applications to concrete structural elements Comput Method Appl M 2006;195:7264–81.

[31] Oliveira RS, Ramalho MA, Corrêa MRS. A layered finite element for reinforced concrete beams with bond-slip effects. Cement Concrete Comp 2008;30:245–52.

[32] Jones J, Wua C, Oehlers DJ, Whittaker AS, Sunc W, Marksa S, Coppola R. Finite difference analysis of simply supported RC slabs for blast loadings. Eng Struct 2009;31(12):2825–32.

[33] Chandrasekaran S., Nunziante L, Serino G, Carannante F. Curvature Ductility of RC Sections Based on Eurocode: Analytical Procedure. KSCE J Civ Eng 2011;15(1):131–44.

[34] Daniell JE, Oehlers DJ, Griffith MC, Mohamed Ali MS, Ozbakkaloglu T. The softening rotation of reinforced concrete members. Eng Struct 2008;30(11):3159–66.

[35] Haskett M, Oehlers DJ, Mohamed Ali MS, Wu C. Rigid body moment-rotation mechanism for reinforced concrete beam hinges. Eng Struct 2009;31(5):1032–41.

[36] EN 1992-1-1, Eurocode 2: Design of concrete structures - Part 1-1: General rules and rules for buildings; 2004.

[37] International Federation for Structural Concrete (*fib*), Constitutive modelling of high strength/high performance concrete. State-of-art report. *fib* Bulletin 42; 2008.

[38] Jirásek M, Bazant ZP. Models for Localization of Softening and Size Effect. In: Inelastic Analysis of Structures. Chichester: John Wiley and Sons; 2002, p. 517–39.

[39] Challamel N, Hjiaj M. Non-local behaviour of plastic softening beams. Acta Mech 2005;178(3-4):125–46.

[40] Géradin M, Rixen D. Mechanical vibrations: theory and application to structural dynamics. Paris: Masson; 1994.

[41] Diamonds 2010 r.01. Buildsoft NV; http://www.buildsoft.eu.

[42] Smith PD, Hetherington JG. Blast and ballistic loading of structures. London: Butterworth Heinemann; 1994.

[43] Priestley MJN, Seible F. Design of seismic retrofit measures for concrete and masonry structures. Constr Build Mater 1995;9(6):365–77.

[44] Bischoff PH, Perry SH. Compressive Behaviour of Concrete at High Strain Rates. Mater Struct 1991;24:425–50.

[45] Malvar LJ, Crawford JE. Dynamic increase factors for concrete. 28th DDESB seminar. Orlando, FL, USA; 1998.

[46] Grote DL, Park SW, Zhou M. Dynamic behaviour of concrete at high strain rates and pressures: I. experimental characterization. Int J Impact Eng 2001;25:869–86.

[47] Li QM, Meng H. About the dynamic strength enhancement of concrete-like materials in a split Hopkinson pressure bar test. Int J Solids Struct 2003;40:343–60.

[48] Malvar LJ, Crawford JE. Dynamic increase factors for steel reinforcing bars. 28th DDESB seminar. Orlando, FL, USA; 1998.

[49] Pedersen RR, Simone A, Sluys LJ, An analysis of dynamic fracture in concrete with a continuum visco-elastic visco-plastic damage model. Eng Fract Mech 2008;75:3782–3805.

[50] Georgin JF, Reynouard JM. Modeling of structures subjected to impact: concrete behaviour under high strain rate. Cement Concrete Comp 2003;25:131–43.

[51] Lorefice R, Etse G, Carol I. Viscoplastic approach for rate-dependent failure analysis of concrete joints and interfaces. Int J Solids Struct 2008;45;2686–2705.

[52] Abbas H, Gupta NK, Alam M. Nonlinear response of concrete beams and plates under impact loading. Int J Impact Eng 2004;30:1039–53.

[53] de Borst R, Sluys LJ, Geers MGD. Computational methods for material nonlinearities. Graduate School on Engineering Mechanics. Delft University of Technology. Delft, The Netherlands; 1998.

[54] Heeres OM, Suiker ASJ, de Borst R. A comparison between the Perzyna viscoplastic model and the Consistency viscoplastic model. Eur J Mech A-Solid 2002;21:1–12.

Captions

Fig. 1. Stress-strain curve of the proposed model for concrete in compression.

Fig. 2. Layered beam model: generalised stresses evaluation.

Fig. 3. Five-storey frame under study.

Fig. 4. Description of the RC beams sections (values in mm).

Fig. 5. **Case A**: response of the reference structure to a sudden column removal.

Fig. 6. **Case B**: response for $\epsilon_{c,lim}$ = -0.5%.

Fig. 7. **Case C**: response for $\epsilon_{s,lim}$ = 10%.

Fig. 8. **Case D**: response for $\epsilon_{c,lim}$ = -0.5% and $\epsilon_{s,lim}$ = 10%.

Fig. 9. **Case E**: response for 50% increased reinforcement.

Fig. 10. **Case F**: response for a column removal time t_r = 500 ms.

Fig. 11. Vertical displacement of the node on top of the removed column as a function of: (a) the material parameters; (b) the reinforcement amount; (c) the removal time.
(a)
(b)
(c)

Fig. 12. **Case G**: response to the sudden loss of an interior column.

Fig. 13. **Case H**: response to the DoD approach (50% of the live loads).

Fig. 14. **Case I**: response to the DoD approach for an interior column removal.

Fig. 15. Vertical displacement of the node on top of the removed column as a function of the analysis procedure (GSA vs. DoD).
(a) exterior column loss
(b) interior column loss

Fig. 16. Rate-dependent response of the proposed model.
(a) concrete in compression
(b) steel

Fig. 17. Dynamic increase factors.
(a) concrete in compression [45]
(b) steel [48]

Fig. 18. Rate dependent constitutive parameters.
(a) Young's modulus $E_c(\dot{\epsilon})$ in concrete.
(b) Viscoplastic parameter η_c in concrete.
(c) Viscoplastic parameter η_s in steel.

Fig. 19. Rate dependent response for a column removal time of $t_r = 5$ ms.

Fig. 20. Rate dependent response for a removal time $t_r = 500$ ms.

Fig. 21. Vertical displacement of the node on top of the removed column: rate dependent vs. rate independent approach

Figures&Captions

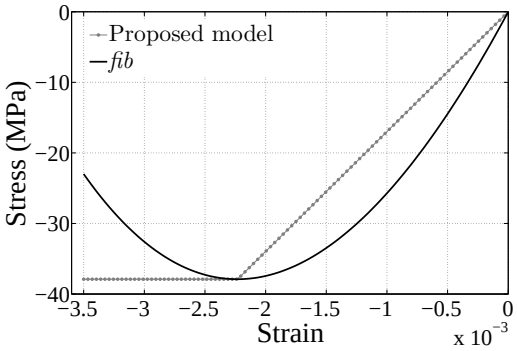

Fig. 1. Stress-strain curve of the proposed model for concrete in compression.

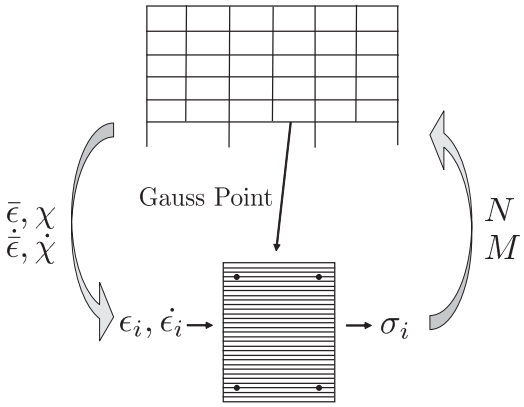

Fig. 2. Layered beam model: generalised stresses evaluation.

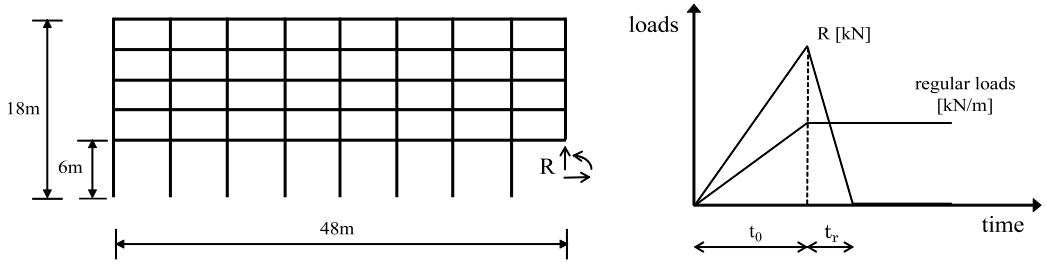

Fig. 3. Five-storey frame under study.

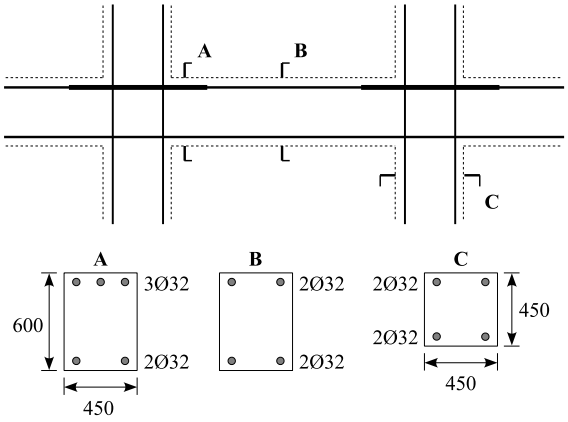

Fig. 4. Description of the RC beams sections (values in mm).

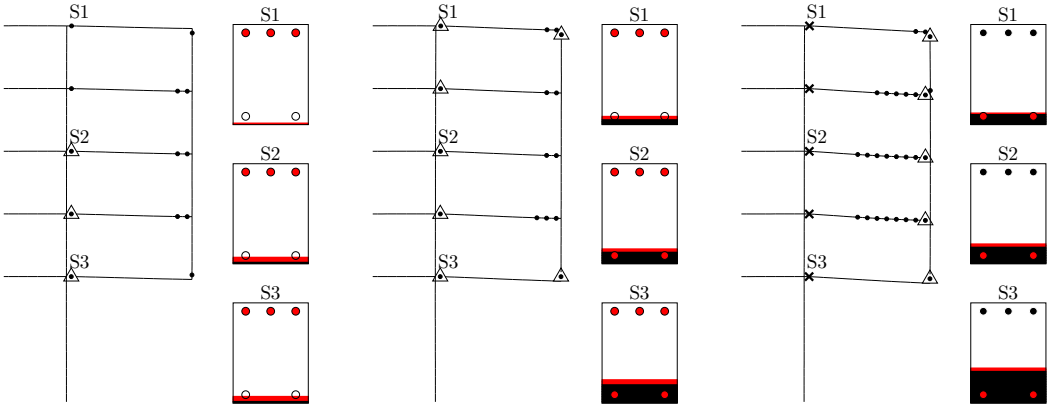

(a) after 200 ms (b) after 300 ms (c) after 420 ms

Fig. 5. **Case A**: response of the reference structure to a sudden column removal.

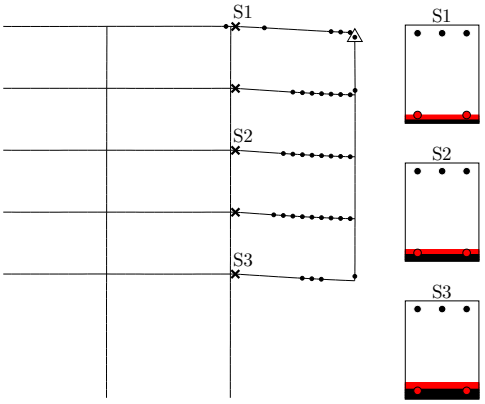

after 430 ms

Fig. 6. **Case B**: response for $\epsilon_{c,lim}$ = -0.5%.

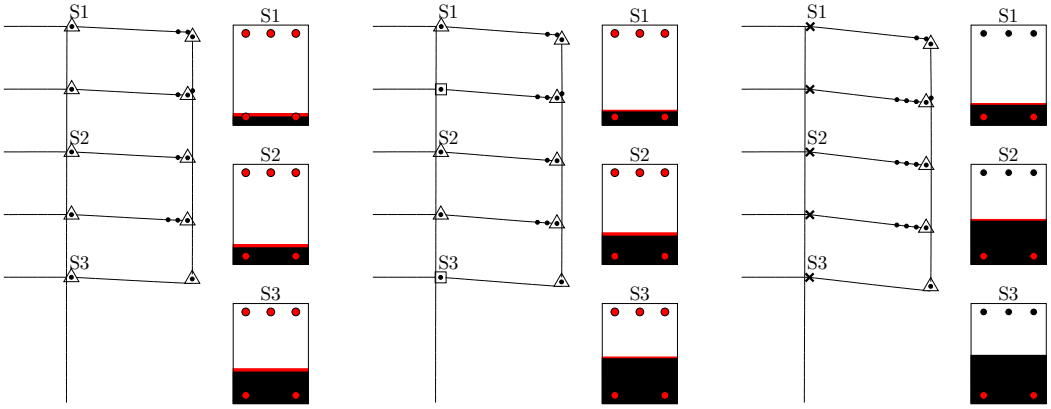

(a) after 400 ms (b) after 600 ms (c) after 885 ms

Fig. 7. **Case C**: response for $\epsilon_{s,lim} = 10\%$.

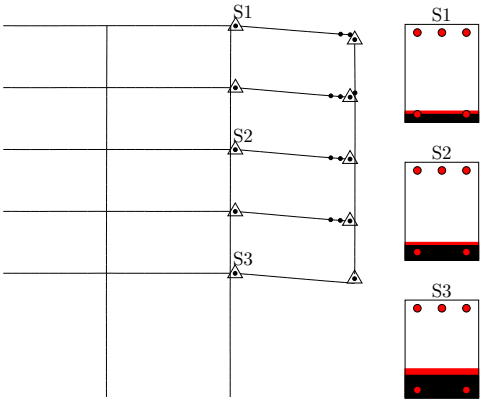

after 2000 ms

Fig. 8. **Case D**: response for $\epsilon_{c,lim}$ = -0.5% and $\epsilon_{s,lim} = 10\%$.

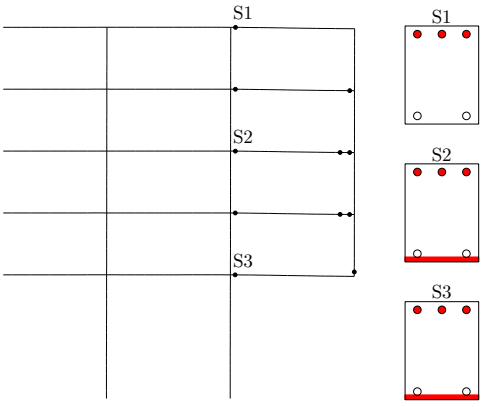

after 2000 ms

Fig. 9. **Case E**: response for 50% increased reinforcement.

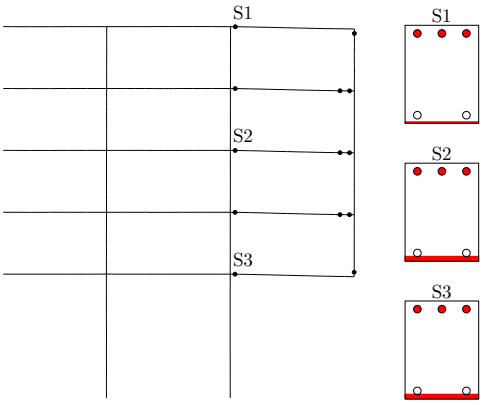

Fig. 10. **Case F**: response for a column removal time $t_r = 500$ ms.

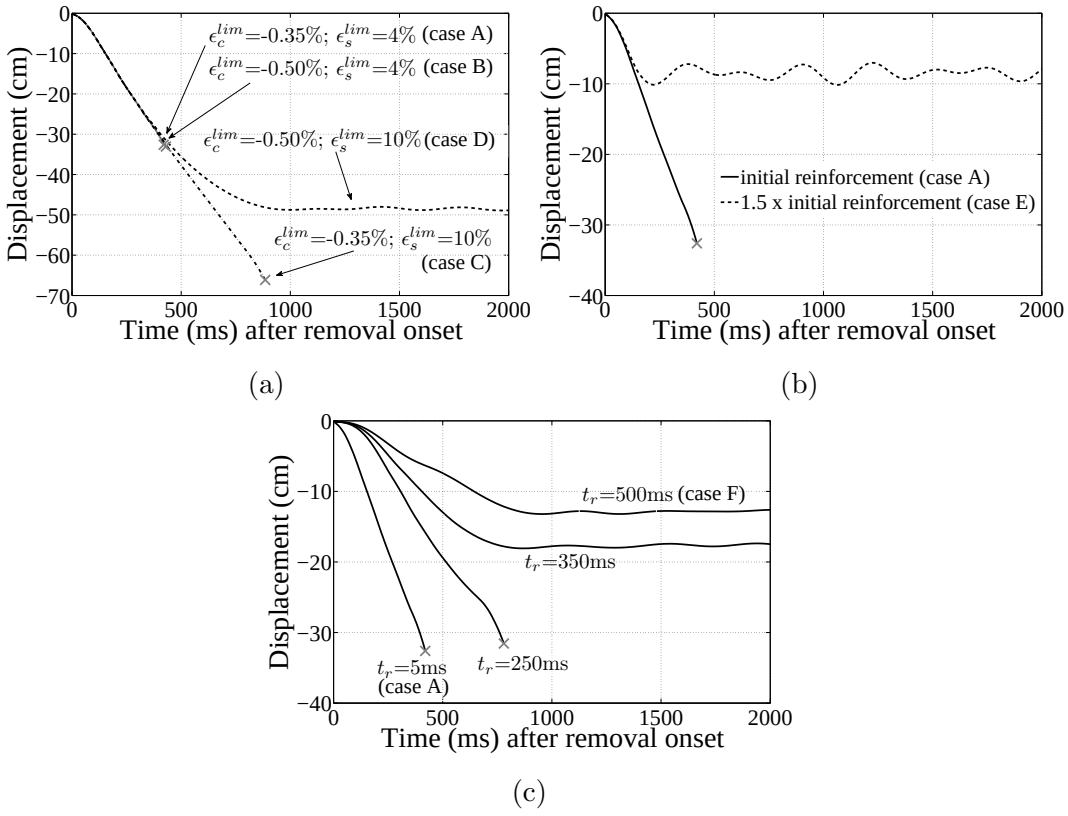

Fig. 11. Vertical displacement of the node on top of the removed column as a function of: (a) the material parameters; (b) the reinforcement amount; (c) the removal time.

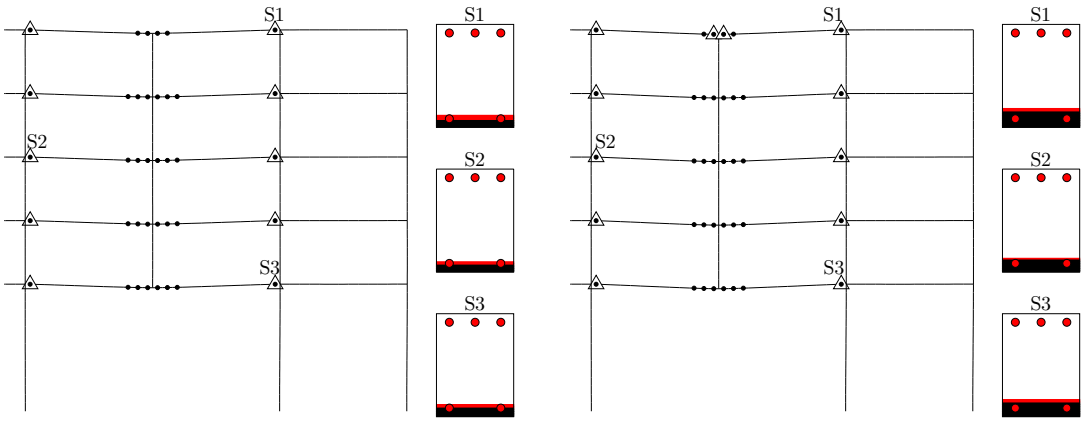

(a) after 300 ms (b) after 2000 ms

Fig. 12. **Case G**: response to the sudden loss of an interior column.

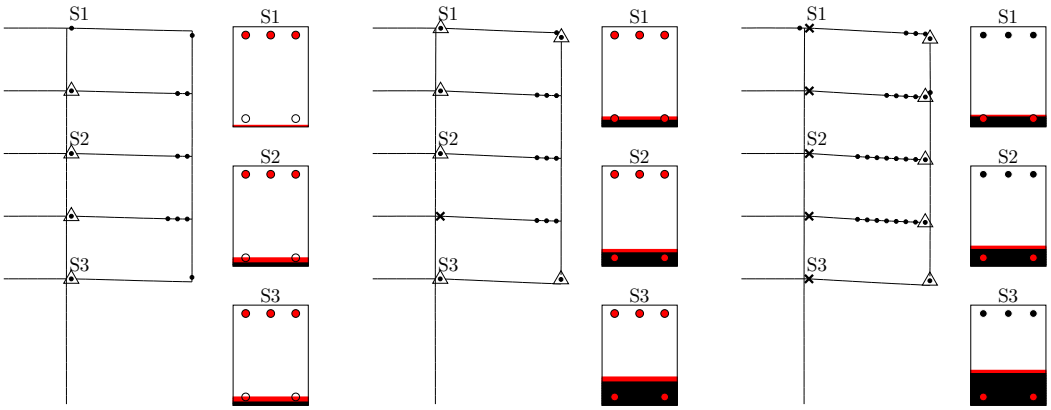

(a) after 200 ms (b) after 300 ms (c) after 365 ms

Fig. 13. **Case H**: response to the DoD approach (50% of the live loads).

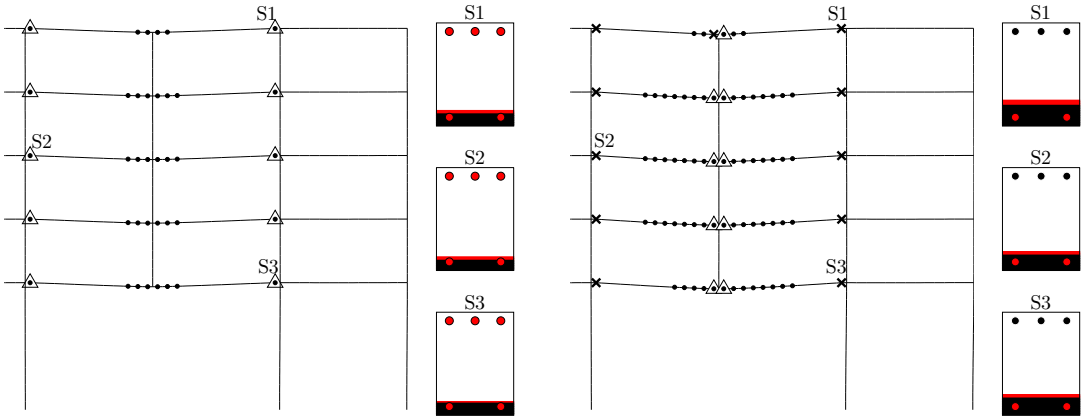

(a) after 300 ms (b) after 450 ms

Fig. 14. **Case I**: response to the DoD approach for an interior column removal.

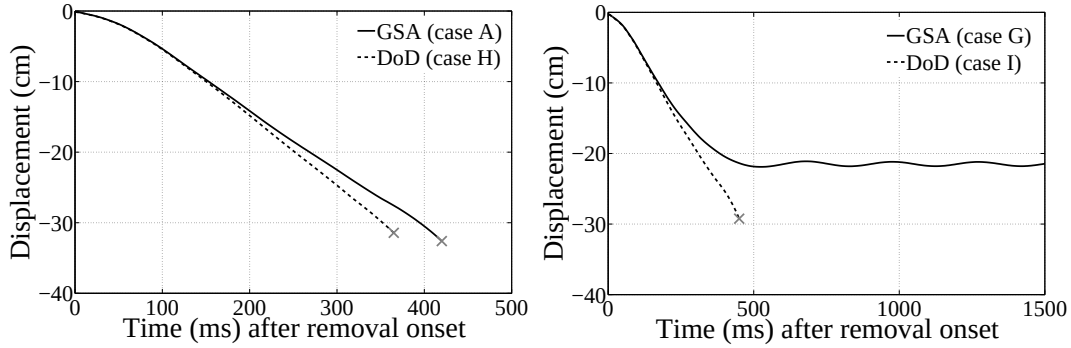

(a) exterior column loss (b) interior column loss

Fig. 15. Vertical displacement of the node on top of the removed column as a function of the analysis procedure (GSA vs. DoD).

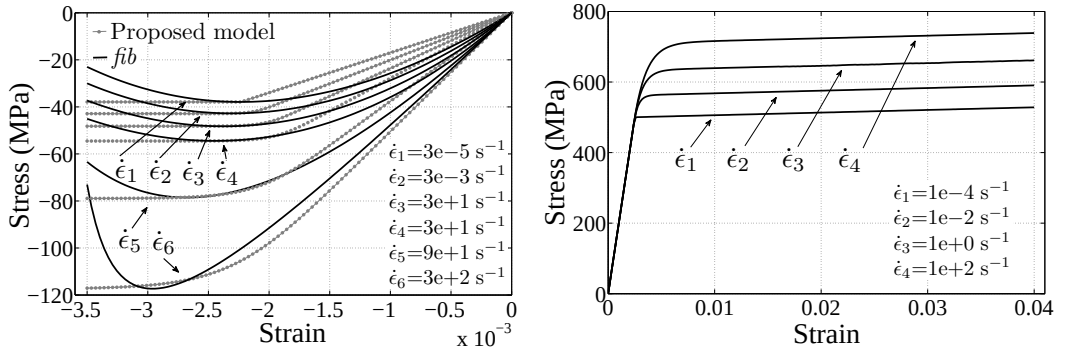

(a) concrete in compression (b) steel

Fig. 16. Rate-dependent response of the proposed model.

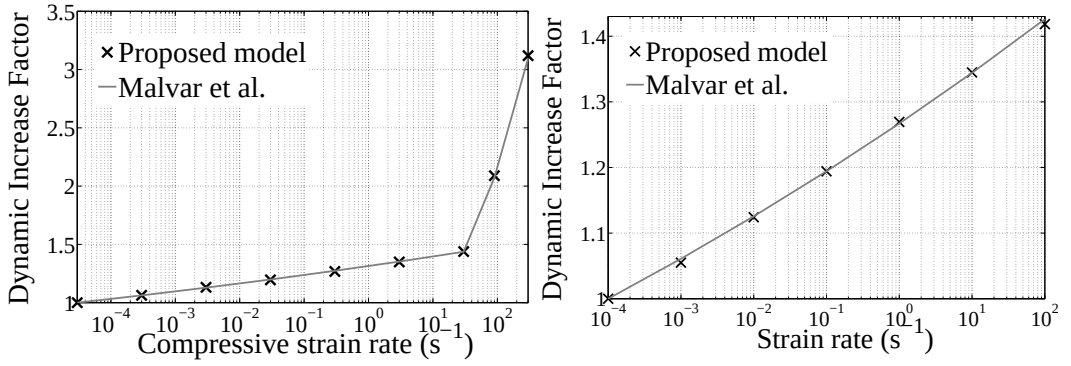

(a) concrete in compression [45] (b) steel [48]

Fig. 17. Dynamic increase factors.

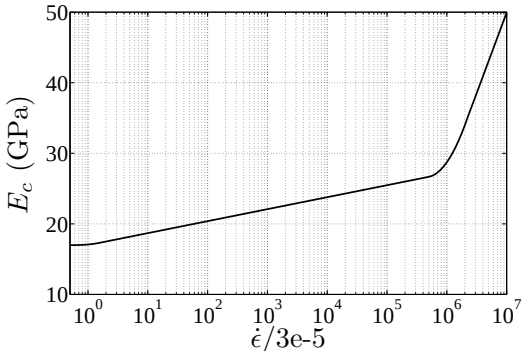

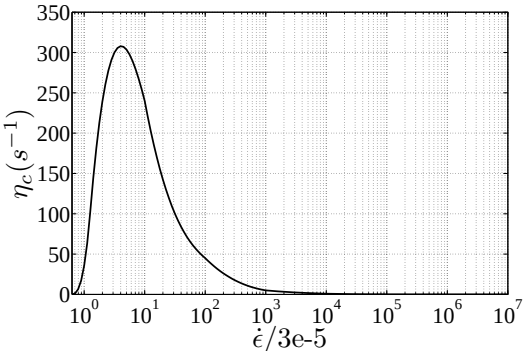

(a) Young's modulus $E_c(\dot{\epsilon})$ in concrete. (b) Viscoplastic parameter η_c in concrete.

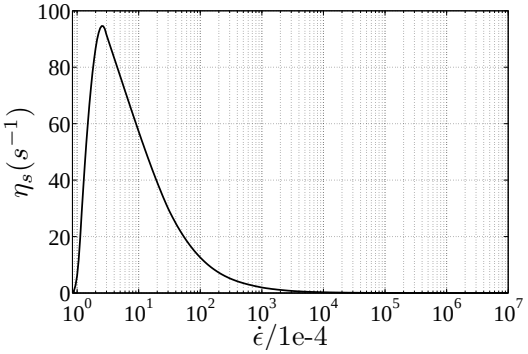

(c) Viscoplastic parameter η_s in steel.

Fig. 18. Rate dependent constitutive parameters.

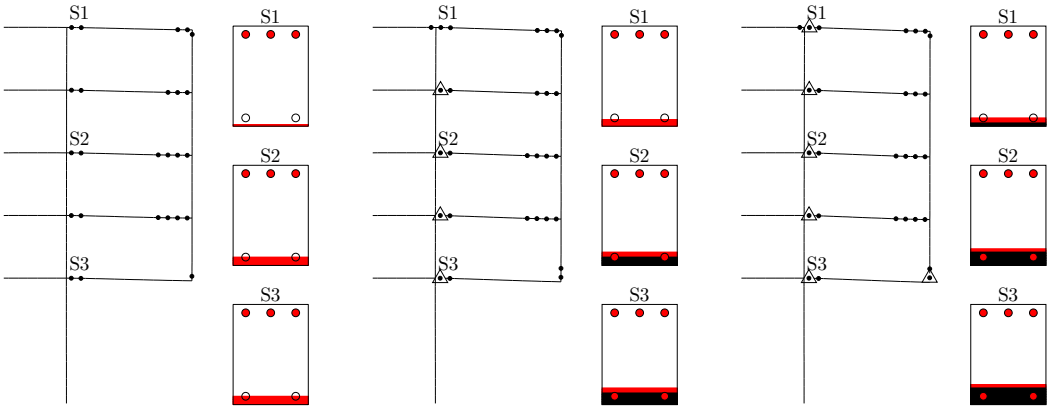

(a) after 200 ms (b) after 300 ms (c) after 2000 ms

Fig. 19. Rate dependent response for a column removal time of $t_r = 5$ ms.

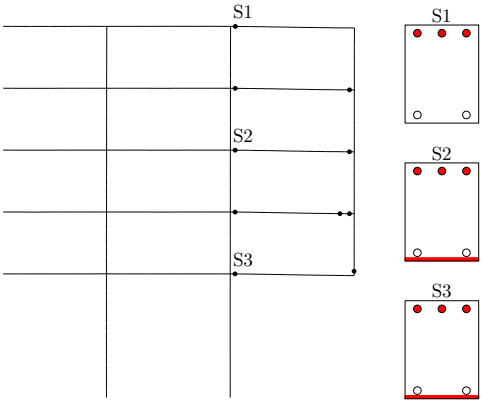

after 2000 ms

Fig. 20. Rate dependent response for a removal time $t_r = 500$ ms.

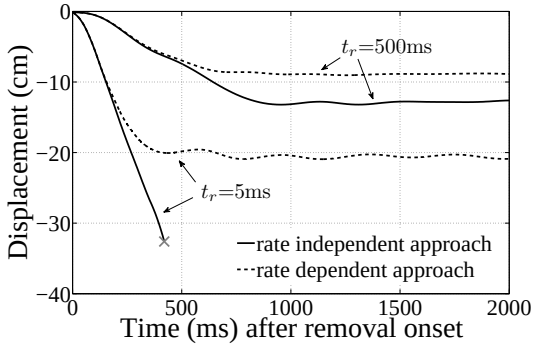

Fig. 21. Vertical displacement of the node on top of the removed column: rate dependent vs. rate independent approach